A GENETIC ALGORITHM APPROACH TO THE DESIGN OF ULTRA-THIN ELECTROMAGNETIC BANDGAP ABSORBERS

D. J. Kern and D. H. Werner
Department of Electrical Engineering
Pennsylvania State University
University Park, PA 16802 USA

Received 11 December 2002

ABSTRACT: *A design methodology is presented for utilizing electromagnetic bandgap metamaterials, also known as artificial magnetic conductors, to realize ultra-thin absorbers. One approach that has recently been proposed is to place a resistive sheet in close proximity to a frequency-selective surface acting as an artificial magnetic conductor. However, we demonstrate in this paper that incorporating the loss directly into the frequency selective-surface can eliminate the additional resistive sheet, thereby further reducing the overall thickness of the absorber. The geometrical structure and corresponding resistance of this lossy frequency-selective surface is optimized by using a genetic algorithm to achieve the thinnest possible absorber. Two examples of genetically engineered electromagnetic bandgap metamaterial absorbers are presented and discussed.* © 2003 Wiley Periodicals, Inc. Microwave Opt Technol Lett 38: 61–64, 2003; Published online in Wiley InterScience (www.interscience.wiley.com). DOI 10.1002/mop.10971

Key words: *electromagnetic bandgap; metamaterial; artificial magnetic conductor; frequency-selective surface; ultra-thin absorber*

1. INTRODUCTION

In many radar and tracking applications, it is desirable to control the enhancement or reduction of the radar cross section (RCS) of an object. A typical method of reducing the RCS of a structure is to coat the surface with some type of lossy material that can increase the absorption of electromagnetic waves at the operating frequency of the radar [1–3]. To this end, there has been a considerable amount of interest over the years in the development of new design methodologies for lightweight, ultra-thin absorber coatings.

One of the most popular classical electromagnetic absorber design techniques is based on the use of so-called Salisbury screens [4]. This structure consists of a resistive metallic screen placed a quarter-wavelength above a ground plane, separated by a dielectric. The resistive metallic screen reflects a portion of the incident electromagnetic wave, while the remaining part travels through the dielectric and is reflected off the ground plane. At the resonant frequency of the Salisbury screen, the phase difference between the two reflected waves is equal to 180°, and thus the two waves cancel. The distance the lossy screen is placed above the conductor backing therefore determines the absorbing frequency. An illustration of such an absorber along with its frequency response is shown in Figure 1. One advantage to such a design is the simplicity of the structure, while the main disadvantage is the relatively large thickness of a quarter wavelength, which can severely limit the physical applications of the absorber. Therefore, it is highly desirable to find alternative design approaches that would lead to much thinner absorbers with comparable performance characteristics.

Recently, it has been shown by Engheta [5] that the absorber thickness can be considerably reduced with respect to that of a standard Salisbury screen by using a gangbuster frequency-selective surface (FSS) and a resistive sheet placed above the ground plane [5]. A gangbuster FSS consists of a series of closely spaced

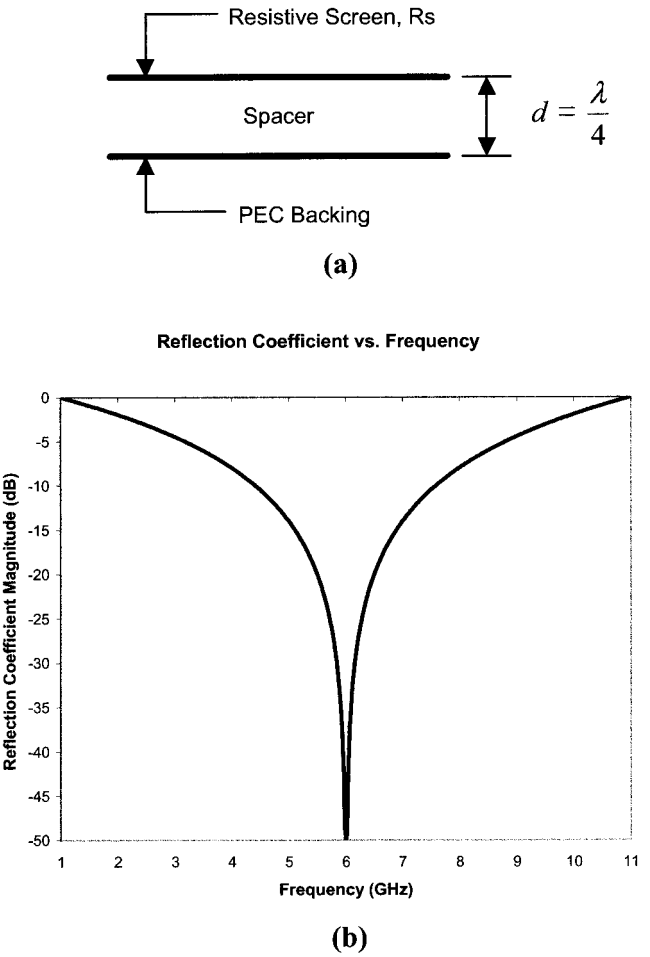

Figure 1 Single-layer Salisbury screen geometry and corresponding plot of the frequency response: (a) geometry of standard Salisbury screen; and (b) frequency response for sheet resistance $R_s = 377\Omega$

dipole elements arranged periodically to form the screen [6]. When the FSS is placed close to the conductor backing, the structure acts as a high-impedance frequency-selective surface (HZ FSS) or artificial magnetic conductor (AMC) over a narrow frequency band. In this case, a resistive sheet was used to provide the necessary loss, and was placed just above the FSS screen.

The designs presented here demonstrate their ability to reduce the complexity and thickness of the gangbuster FSS design by replacing the resistive sheet and gangbuster FSS with a single lossy HZ FSS screen. In this case, the HZ FSS geometry is more general than that of the gangbuster FSS and can be optimized according to the desired operating frequency. These designs still retain high-impedance properties at or near the absorbing frequency where the phase of the reflection coefficient is 0°. These new HZ FSS absorber designs therefore combine the advantages of an AMC structure with those of a thin resistive screen. Furthermore, the resistive HZ FSS allows for considerably thinner designs, compared to that of a Salisbury screen or other conventional methods.

2. GENETIC ALGORITHM APPROACH

In this section an optimization methodology is introduced for synthesizing ultra-thin electromagnetic bandgap absorbers via lossy HZ FSS. Due to the complex nature of the problem, conventional optimization methods were not considered in favor of a

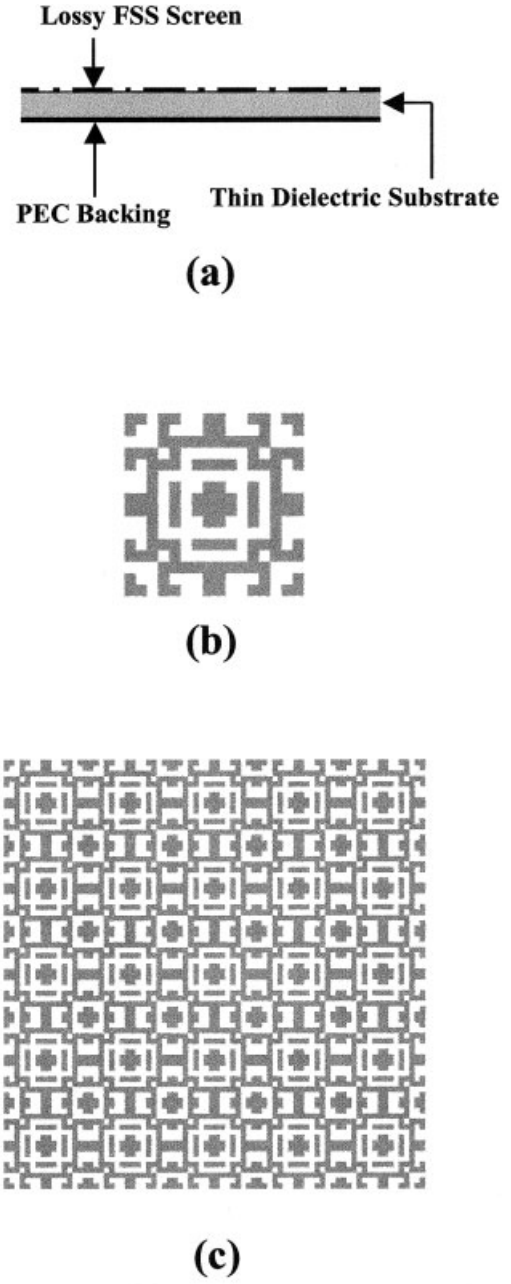

Figure 2 Resistive FSS absorber structure and screen geometry for operation at 6 GHz: (a) general resistive FSS absorber configuration; (b) unit cell geometry for λ/10 design; and (c) FSS screen geometry for λ/10 design

more robust genetic algorithm (GA) approach. A similar GA technique was previously employed in [7] to successfully synthesize optimal HZ FSS designs for multi-band AMC surfaces. The use of a GA allows for simultaneous optimization of the unit-cell size, dielectric permittivity and thickness, and FSS screen geometry, as well as the resistive component of the FSS screen. The result is a robust optimization procedure that can be used to design an ultra-thin resistive FSS structure with an AMC and absorbing properties at the desired frequency. Due to the rather long convergence time that would be required for a conventional GA, a micro-GA was used in the actual optimization procedure. A micro-GA optimizes on a much smaller population of chromosomes, which considerably reduces the overall computation time needed to reach convergence [8]. The fitness function (FF) used in the micro-GA for synthesizing a lossy HZ FSS is given by

$$FF = \frac{1}{0.2|\phi_{\max}/180| + 0.8|\Gamma_{\max}|,} \tag{1}$$

where $|\Gamma_{\max}|$ and $\phi_{\max}$ are the maximum reflection coefficient magnitude and phase respectively. As can be seen from Eq. (1), it was found that better convergence was achieved by placing greater weight on the magnitude of the reflection coefficient.

3. ULTRA-THIN ABSORBER DESIGN EXAMPLES

Two examples of genetically engineered ultra-thin electromagnetic bandgap absorbers will be presented and discussed in this section. The objective in the first case is to design an absorber centered at 6 GHz with a maximum dielectric substrate thickness of 5 mm, or about a tenth of a wavelength. The GA was used to synthesize a design with a unit cell size of 2.73 cm by 2.73 cm, a screen

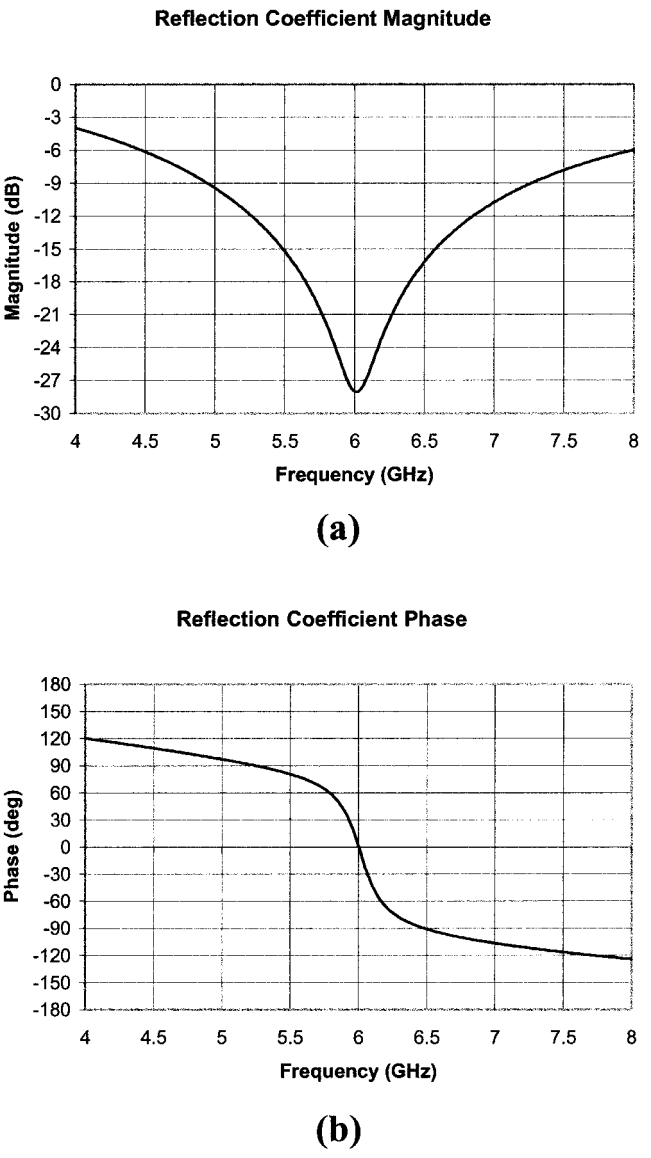

Figure 3 Reflection coefficient vs. frequency response for λ/10 design: (a) magnitude of the reflection coefficient vs. frequency; and (b) phase of the reflection coefficient vs. frequency

resistance of about 84Ω, and a substrate permittivity of $\varepsilon_r = 6$. The FSS structure, including unit cell and screen geometry, is shown in Figure 2. The magnitude and phase of the reflection coefficient for this FSS are shown in Figure 3, assuming a normally incident electromagnetic plane wave. It can be seen from Figure 3(b) that the phase of the reflection coefficient at 6 GHz is 0°, indicating the high-impedance behavior of the resistive FSS.

While the tenth of a wavelength thickness yielded very good absorbing characteristics at the desired operating frequency, for certain applications this structure may still be considered too thick. As such, a second design example was synthesized via the GA, again for operation at 6 GHz. This time, however, the maximum substrate thickness was fixed at 1 mm, which corresponds to approximately one-fiftieth of a wavelength. The optimal unit cell size in this case was found to be 3.54 cm by 3.54 cm, with a permittivity of $\varepsilon_r = 1.044$. The actual substrate thickness of the optimized structure was 0.952 mm, with an FSS screen resistance of 0.7Ω. The unit cell and FSS screen geometry are shown in Figure 4. The reflection coefficient magnitude and phase plots for this design are shown in Figure 5. A comparison of Figures 5 and 3 indicates that the thinner of the two absorbers has the narrower bandwidth.

4. CONCLUSION

A robust GA optimization approach has been introduced for the synthesis of ultra-thin electromagnetic bandgap metamaterial absorbers. Two examples of these genetically engineered absorbers have been presented, which are considerably thinner than more conventional absorber designs, such as Salisbury screens. It was also demonstrated that the overall thickness of the metamaterial absorber can be reduced by incorporating the loss directly into the FSS, rather than placing a separate resistive sheet in close proximity to the FSS.

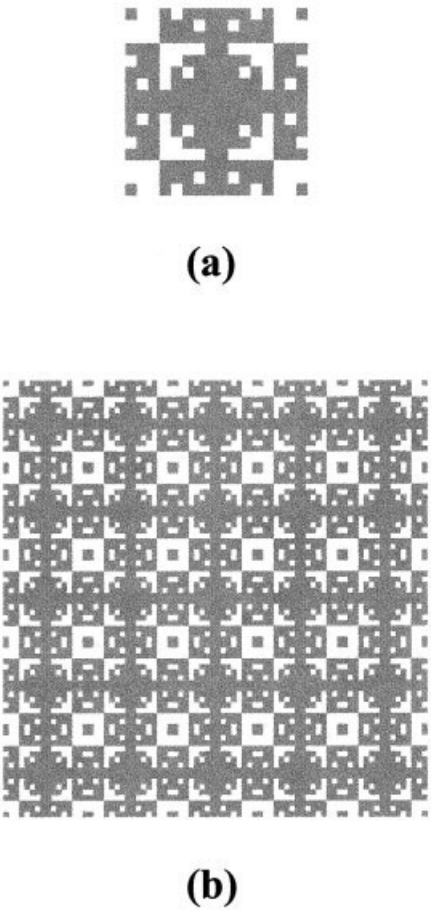

Figure 4 Resistive FSS geometry for λ/50 design: (a) unit cell geometry for λ/50 design; and (b) resistive FSS screen geometry for λ/50 design

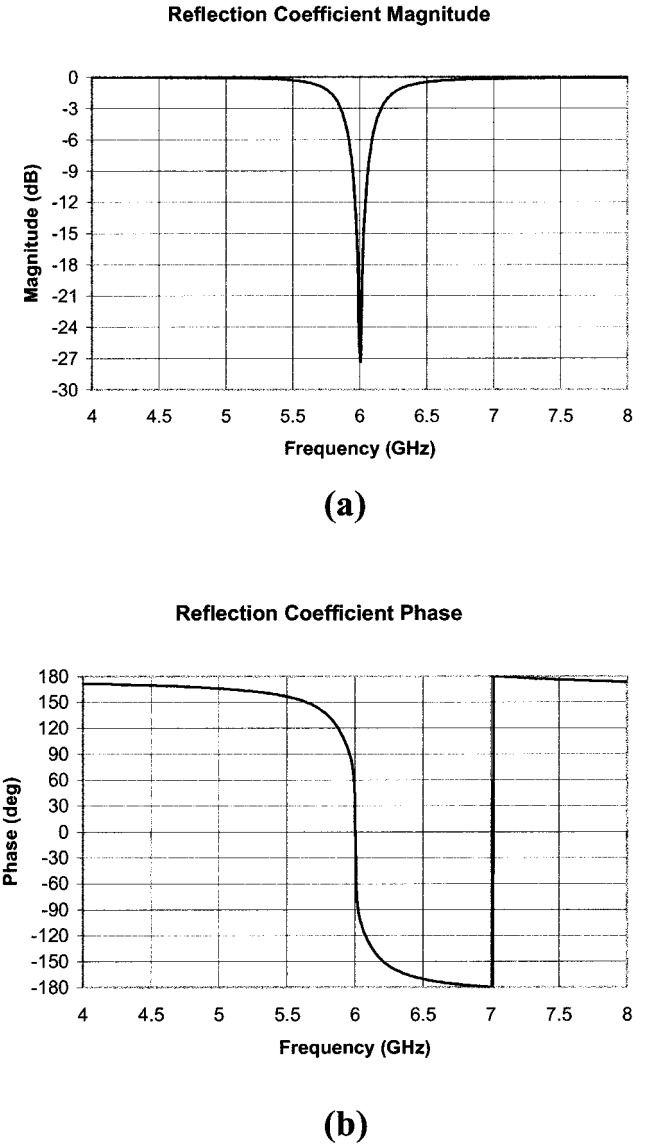

Figure 5 Reflection coefficient vs. frequency response for λ/50 design: (a) magnitude of the reflection coefficient vs. frequency; and (b) phase of the reflection coefficient vs. frequency

REFERENCES

1. A.K. Bhattacharyya and D.L. Sengupta, Radar cross section analysis and control, Artech House, Boston, 1991.
2. K.J. Vinoy and R.M. Jha, Radar absorbing materials: From theory to design and characterization, Kluwer, Boston, 1996.
3. G.T. Ruck, D.E. Barrick, W.D. Stuart, and C.K. Krichbaum, Radar cross section handbook, vol. 2, Plenum, New York, 1970, pp. 611–629.
4. R.L. Fante and M.T. McCormack, Reflection properties of the Salisbury screen, IEEE Trans Antennas Propagat 36 (1988), 1443–1454.
5. N. Engheta, Thin absorbing screens using metamaterial surfaces, Proc IEEE AP-S/URSI Symp Dig, 2002, pp. 392–395.
6. B.A. Munk, Frequency selective surfaces: Theory and design. Wiley, New York, 2000, pp. 28–32.

7. D.J. Kern, D.H. Werner, M.J. Wilhelm, K.H. Church, and R. Mittra, Multi-band high impedance frequency selective surfaces, in Proc IEEE AP-S/URSI Symp Dig, June 2002, URSI Digest, p. 264.
8. G. Dozier, J. Bowen, and D. Bahler, Solving small and large scale constraint satisfaction problems using a heuristic-based microgenetic algorithm, in Proc IEEE Intl Conf Evolutionary Comp, June 1994, vol. 1, pp. 306–311.

COUPLING MATRIX OF A 10TH-ORDER DUAL-MODE ASYMMETRIC CANONICAL FILTER

Juseop Lee, Man Seok Uhm, In-Bok Yom, and Seong Pal Lee
Communications Satellite Development Center
Electronics and Telecommunications Research Institute (ETRI)
161, Gajeong-dong, Yuseong-gu
Daejeon, 305-350, South Korea

Received 9 December 2002

ABSTRACT: *This paper deals with a simple method to extract the coupling matrix of a 10th-order dual-mode asymmetric canonical filter. The coupling matrix of an asymmetric canonical filter is obtained by applying a plane rotation technique to the coupling matrix of a symmetric canonical filter. This paper gives a list of pivots and rotation angles to obtain the coupling matrix of an asymmetric canonical-structure filter.*
 Microwave Opt Technol Lett 38: 64–68, 2003; Published online in Wiley InterScience (www.interscience.wiley.com). DOI 10.1002/mop.10972

Key words: *dual-mode filter; canonical filter; coupling matrix*

1. INTRODUCTION

With the advent of the dual-mode elliptic response filter [1], satellite transponders have become smaller with less mass than conventional ones. Furthermore, due to the elliptic response characteristic of the channel filter, the frequency spectrum can be used more efficiently.

Due to ease of fabrication, the longitudinal dual-mode filter, with input and output ports positioned on opposite sides of the structure, has been studied and designed widely [2, 3], including a filter without tuning screws [4, 5] and a DR-loaded filter [6]. However, as described in [7], the longitudinal dual-mode filter has the drawback that its physical restriction results in the reduction of the number of finite zeros of transmission that can be generated in the filter's transfer function.

A possible configuration to overcome this problem is the canonical form [7]. Symmetric and asymmetric canonical dual-mode filters can be realized by finding their coupling matrix from a rational transfer function. The coupling matrix of a symmetric filter can be easily obtained with a method described in [1], but an asymmetric filter needs lengthy and complicated equations to obtain its coupling matrix, especially for the higher-order filter case. Therefore, this paper describes a method to obtain a coupling matrix of an asymmetric canonical filter from that of a symmetric canonical filter by using a plane rotation technique.

2. THEORY

Figure 1 shows a lumped circuit representation of an n^{th}-order doubly terminated filter. The transfer function of the doubly terminated filter can generally be expressed as the following rational function:

$$t(s) = S_{21}(s) = \frac{1}{\varepsilon}\frac{P(s)}{E(s)}. \tag{1}$$

From the lumped circuit representation, the relationship between current and voltage can be obtained and expressed by the following matrix form [8]:

$$[\omega U - jR + M][I] = [A][I] = -j[e], \tag{2}$$

where U is an $n \times n$ identity matrix, M is an $n \times n$ mutual coupling matrix, and R is given by

$$[R] = \begin{bmatrix} R_{in} & 0 & \cdots & 0 & 0 \\ 0 & 0 & \cdots & 0 & 0 \\ \vdots & \vdots & \ddots & \vdots & \vdots \\ 0 & 0 & \cdots & 0 & 0 \\ 0 & 0 & \cdots & 0 & R_{out} \end{bmatrix}. \tag{3}$$

The excitation vector $[e]$ is given by $[e]^t = [1 \quad 0 \quad \cdots \quad 0]$ where t is the transposition operator of the matrix. Since, from Eq. (2), the vector current $[I]$ is given by

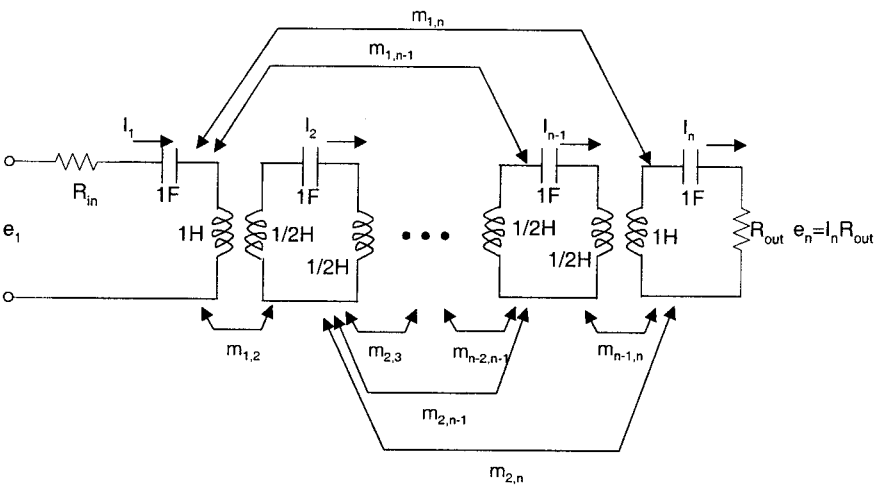

Figure 1 n^{th}-order synchronously tuned doubly terminated filter